

An extended defect as a sensor for free carrier diffusion in a semiconductor

T. H. Gfroerer, Yong Zhang, and M. W. Wanlass

Citation: *Appl. Phys. Lett.* **102**, 012114 (2013); doi: 10.1063/1.4775369

View online: <http://dx.doi.org/10.1063/1.4775369>

View Table of Contents: <http://apl.aip.org/resource/1/APPLAB/v102/i1>

Published by the [American Institute of Physics](#).

Related Articles

Coupling characteristics of point defects modes in two-dimensional magnonic crystals
J. Appl. Phys. **112**, 103911 (2012)

A reaction diffusion model of pattern formation in clustering of adatoms on silicon surfaces
AIP Advances **2**, 042101 (2012)

Convergent beam electron-diffraction investigation of lattice mismatch and static disorder in GaAs/GaAs_{1-x}N_x intercalated GaAs/GaAs_{1-x}N_x:H heterostructures
Appl. Phys. Lett. **101**, 111912 (2012)

Response to "Comment on 'Elastic wave propagation in a solid layer with laser-induced point defects'" [*J. Appl. Phys.* **112**, 056101 (2012)]
J. Appl. Phys. **112**, 056102 (2012)

Comment on "Elastic wave propagation in a solid layer with laser-induced point defects" [*J. Appl. Phys.* **110**, 064906 (2011)]
J. Appl. Phys. **112**, 056101 (2012)

Additional information on *Appl. Phys. Lett.*

Journal Homepage: <http://apl.aip.org/>

Journal Information: http://apl.aip.org/about/about_the_journal

Top downloads: http://apl.aip.org/features/most_downloaded

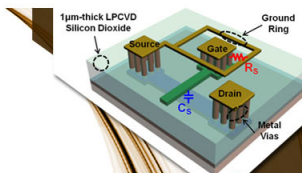
Information for Authors: <http://apl.aip.org/authors>

ADVERTISEMENT



**EXPLORE WHAT'S
NEW IN APL**

SUBMIT YOUR PAPER NOW!



SURFACES AND INTERFACES

Focusing on physical, chemical, biological, structural, optical, magnetic and electrical properties of surfaces and interfaces, and more...



ENERGY CONVERSION AND STORAGE

Focusing on all aspects of static and dynamic energy conversion, energy storage, photovoltaics, solar fuels, batteries, capacitors, thermoelectrics, and more...

An extended defect as a sensor for free carrier diffusion in a semiconductor

T. H. Gfroerer,^{1,2} Yong Zhang,² and M. W. Wanlass³

¹Davidson College, Davidson, North Carolina 28035, USA

²University of North Carolina at Charlotte, Charlotte, North Carolina, USA

³National Renewable Energy Laboratory, Golden, Colorado 80401, USA

(Received 14 September 2012; accepted 20 December 2012; published online 11 January 2013)

We use confocal photoluminescence microscopy to study carrier diffusion near an isolated extended defect (ED) in GaAs. We observe that the carrier diffusion length varies non-monotonically with carrier density, which we attribute to competition between point defects and the extended defect. High density laser illumination induces a permanent change in the structure of the extended defect, more significantly an apparent change in the effective polarity of the defect, and thus a drastic change in its range of influence. The inferred switch of principal diffusing species leads to a potential design consideration for high injection optoelectronic devices. © 2013 American Institute of Physics. [<http://dx.doi.org/10.1063/1.4775369>]

When free electrons and holes are photogenerated in a semiconductor, they naturally diffuse to lower-density regions. If an extended defect (ED) creates a high density of defect levels between the valence and conduction bands, carriers can be captured into these localized states and subsequently recombine. Defect-related trapping and recombination deplete the bands in the vicinity of the dislocation, triggering diffusion to the site. But real semiconductors always host a collection of native and impurity-related point defects (PDs), which tend to be distributed uniformly throughout the bulk. These defects can act as local traps, so long-range transport to an ED only becomes important when bulk defect states are filled. A fundamental understanding of these effects is essential for optimizing opto-electronic device design.

Photoluminescence (PL), cathodoluminescence (CL), and electron-beam-induced current (EBIC) microscopy are powerful techniques for studying EDs like dislocations and the motion of carriers near these crystal imperfections. CL and EBIC produce highly localized carrier populations, which are free to diffuse, drift, and/or recombine, generating luminescence or electric current. But the collection mode of these experiments is usually global—the signal is a combination of contributions from throughout the device. If carrier generation occurs in the vicinity of a dislocation, the net signal is reduced because carriers that would ordinarily contribute to the current or luminescence are captured and recombine at the dislocation. The loss at a distance r is described by the contrast $c(r) = (I_0 - I(r))/I_0$, where I_0 and $I(r)$ are the current or luminescence intensity with the defect absent and present, respectively. This parameter has been analyzed theoretically for a wide variety of geometrical generation and dislocation scenarios.^{1–4} In all cases, the dislocation is treated as a bounded region with an augmented recombination rate (i.e., reduced free carrier lifetime) together with ordinary Laplacian diffusion throughout the neighboring bulk.

The physics of the confocal experiment is unique because the signal is obtained only from a well-defined volume. For example, translation of the collection aperture can be used to monitor carrier transport away from the excitation position.⁵ In our geometry, the excitation and collection

apertures are aligned, so the PL signal originates only within the illuminated volume. If a nearby dislocation is outside this volume, the signal can only be reduced by a defect-related outward flux and loss of carriers within the volume. Prior work in this field has suggested that the signal can also be diminished by elevated impurity concentrations in the vicinity of the dislocation.⁶ But this situation can be ruled out when the PL spectrum is uniform throughout the mapping area and the contrast profile changes systematically with excitation. If impurities were responsible for reducing the PL signal, they would presumably alter the PL spectrum (as in Ref. 6) and produce a contrast profile that was less sensitive to photoexcitation. Hence, excitation-dependent confocal PL is a better technique for focusing exclusively on transport-related changes in carrier concentrations. This advantage is supplemented by the superior quality of the prototype structure and instrumentation used in this investigation. Dislocations are spaced widely enough, and the spatial resolution and dynamic range of the measurement are high enough to permit a quantitative analysis of defect-driven migration at unprecedented distances from a single ED. We use the ED to probe transport dynamics and show that the long-range PL contrast profile is well-described by a simple exponential function.

The test structure for this study is a nominally lattice-matched GaAs/GaInP double heterostructure grown via metal-organic vapor phase epitaxy (MOVPE) on a semi-insulating GaAs substrate. The sample has a very low as-grown threading dislocation density on the order of 10^3 cm^{-2} . Experiments are conducted at room temperature with a Horiba LabRAM HR confocal Raman microscope. In this system, a $\lambda = 633 \text{ nm}$ HeNe laser is focused by a $100\times$, 0.9 NA objective to a nearly diffraction-limited spot size of approximately $1.22\lambda/\text{NA} = 860 \text{ nm}$ in diameter. Neutral density filters in the laser path are used to control the incident optical power (6.5 mW unfiltered). As noted above, the confocal geometry of the instrument ensures that the PL sample volume coincides with the photoexcitation volume. The PL spectrum is acquired via a CCD detector in a 20 nm window centered at 865 nm. High and low energy PL tails extend beyond this spectral window, especially at high excitation

where Fermi filling becomes important, but the integral of the spectrum in this window provides a good relative measure of the band-to-band recombination occurring within the sample volume. PL maps are obtained by laterally translating the sample under the objective lens with a precise, motorized stage.

Confocal PL maps of an isolated as-grown dislocation are shown in Fig. 1. The radiative efficiency is defined as the ratio of the radiative recombination rate over the total recombination rate. Estimates are based on the assumption that the radiative efficiency approaches unity when the PL signal divided by the laser power attains a maximum,⁷ which occurs when the excitation intensity is near 42 KW/cm^2 . At lower excitation, non-radiative defect-related recombination is significant, while the efficiency at higher excitations may suffer from local heating and/or non-radiative Auger processes.

The maps in Fig. 1 show a steady increase in the effective diffusion length with decreasing excitation, followed by a sharp reduction in diffusion at the lowest excitation. The increase in diffusion with decreasing carrier density can be attributed to the increase in carrier lifetime.^{7,8} At low density, electrons and holes must travel further to find a suitable partner for recombination. In this picture, the abrupt decline in diffusion at the lowest carrier density is surprising. This phenomenon was not observed in previous measurements using spatially uniform excitation and PL imaging.⁷ We note that the departure is accompanied by a steep drop in radiative efficiency (the PL signal falls by a factor of 400 with only a factor of 7 reduction in excitation), indicating that the diffusion process is being hindered by nonradiative defect-related recombination in the bulk.⁹ In this regime, carriers fail to diffuse because they are trapped at evenly distributed PD sites within and just beyond the excitation volume. Long-range

migration becomes feasible only when the photoexcitation is sufficient to saturate the bulk traps.

Prolonged high excitation exposure (1100 KW/cm^2 for 2 s) resulted in a permanent modification of the physical properties of the dislocation shown in Fig. 1, presumably via local heating. We note that a similar phenomenon has been reported in EBIC studies of dislocations in MOVPE GaAs.¹⁰ Confocal PL maps of the altered site under conditions comparable to those in Fig. 1 are presented in another report.⁹ In order to demonstrate reproducibility and display the expanded action range, lower magnification confocal maps of the site under a more limited range of photoexcitation conditions are presented here (see, Fig. 2). The plan-view maps show a dramatic overall darkening of the defect site, with two $10 \mu\text{m}$ long linear extensions tilted 45° relative to the $\{1,1,0\}$ cleavage planes (i.e., aligned along $\langle 100 \rangle$ directions). These changes indicate that dislocation networks have formed. The origin, orientation, and dimensions of the features are identical to the optically induced dark line defects observed by Petroff, Johnston, and Hartman in GaAs/AlGaAs double heterostructures.¹¹ Transmission electron microscopy has shown that these networks originate at isolated as-grown dislocations, which thread through the substrate and epilayers, and propagate via a climb mechanism to form interconnected giant dipoles and dislocation loops.^{11,12} When such dark line defects develop during current injection, they are known to cause rapid degradation in GaAs-based lasers,¹² although the underlying physics has not been explained. The discussion below provides insight on the degradation mechanism. We note that the illumination employed here is below the threshold for dislocation glide along $\langle 110 \rangle$ directions.¹³

The extraordinary increase in diffusion toward the altered defect is striking. How does this optical modification

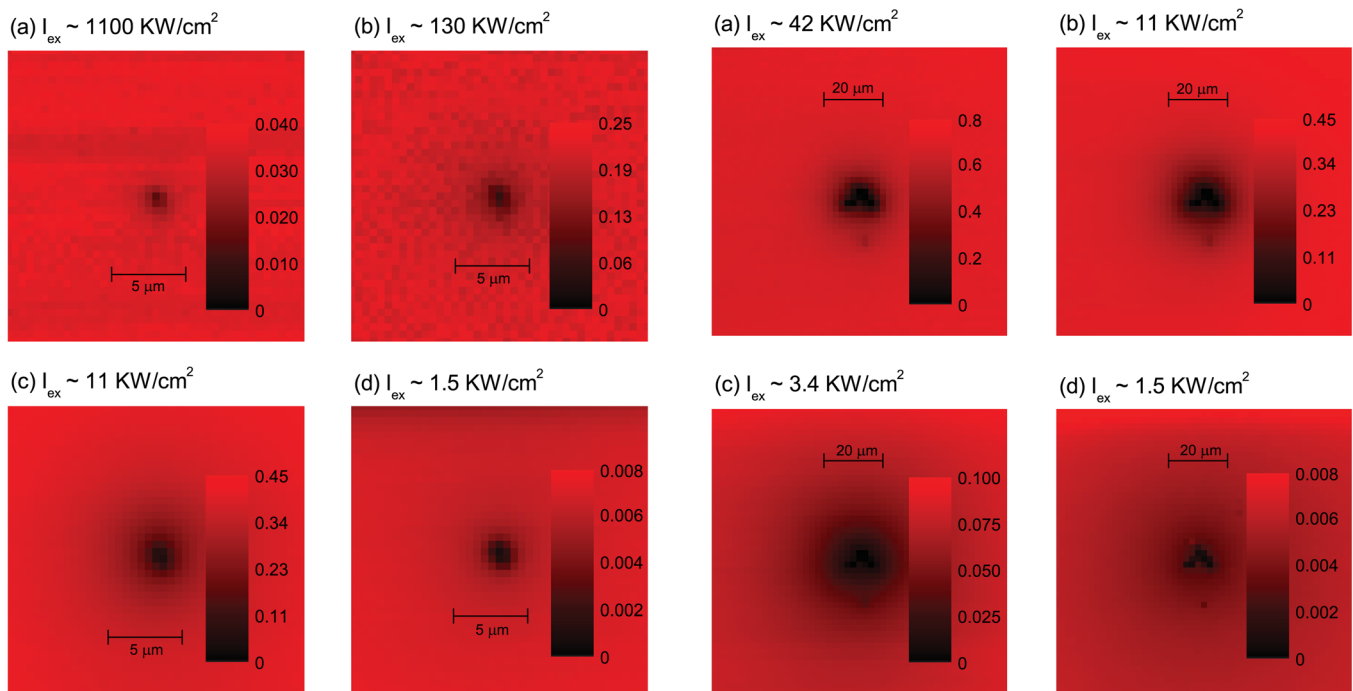


FIG. 1. Plan-view confocal PL maps of an isolated dislocation in GaAs over a wide range of photoexcitation intensities I_{ex} . (I_{ex} values do not include reflection loss.) Greyscale values are estimates of radiative efficiency—the ratio of photons emitted to photons absorbed.

FIG. 2. Plan-view confocal PL maps of the same site examined in Fig. 1 after illumination altered the physical character of the extended defect. Please note the changes in photoexcitation range and magnification relative to those used in Fig. 1.

of the configuration of the defect affect diffusion to the site? The theoretical one-dimensional diffusion length is given by $L = \sqrt{D\tau}$, where D is the diffusion coefficient and τ is the bulk lifetime. Structural deviations can only increase defect-related recombination, so free carrier lifetimes after illumination cannot be longer than the original lifetimes. Therefore, only an increase in D (or a change in electric drift as discussed below) can explain the longer effective diffusion lengths that are observed afterwards. The diffusion coefficient is proportional to the mobility $\mu = e\bar{v}/m^*$, where e is the charge, \bar{v} is the mean scattering time, and m^* is the effective mass of the diffusing species. Presumably, the mean time between scattering events will not become longer with increased material inhomogeneity. This analysis leaves only the effective mass, which is a property of the principal diffusing species, as a viable parameter for explaining our results. Since electron and hole mobilities differ by a factor of 20 in undoped GaAs, we infer that the difference in diffusion is due to a change in the initial carrier being trapped.

An alternative explanation for the change in free carrier motion toward the site is electric drift. If the exposure event changed the electric potential in the vicinity of the defect, the carriers could be drawn in more effectively by the surrounding electric field. The possibility of the presence of charge at dislocations in GaAs has been studied using scanning tunneling microscopy. Cox *et al.*, observed no band bending around the cores indicating that they are electrically neutral,¹⁴ while Ebert, Domke, and Urban reported that partial dislocation cores and the stacking fault between them are negatively charged.¹⁵ However, even in the presence of observed charge, the band bending around the core reaches only a few nanometers into the bulk. We can estimate the extent of the transition region in our system by considering the depletion of background carriers ($N \approx 5 \times 10^{14} \text{ cm}^{-3}$ n-type) in the vicinity of the dislocation network. We find that, even if the Fermi level is pinned to a potential that requires the bands to bend as much as half of the bandgap ($\Delta V = \frac{1}{2}E_g$), the depletion range $W = \sqrt{2\epsilon\Delta V/eN}$ is only approximately $1 \mu\text{m}$. Meanwhile, we observe transport over distances of tens of microns. Hence, while we are reluctant to rule out the possibility that drift contributes to the transport, particularly at short range, we believe that diffusion is the dominant transport mechanism operating in the regime of this investigation.

The PL maps in Figs. 1 and 2 were analyzed using the Radial Profile plug-in on IMAGEJ to obtain plots of the average PL signal as a function of distance from the ED.¹⁶ Contrast profiles derived from these results are shown in Fig. 3. In most cases, the contrast is well-described by a single exponential decay. One notable exception is the lowest excitation result in Fig. 3(b). Unlike the next higher photoexcitation profile, a double exponential is clearly required in this case, as demonstrated in Fig. 4(a). Exponential analysis has been used to model CL contrast near threading dislocations in InGaN/GaN quantum wells¹⁷ and GaN epilayers,¹⁸ but the validity of the exponential description in those experiments has been challenged by Yakimov.¹⁹ In particular, Yakimov argues that the contrast is nonexponential, with the effective diffusion length in the limited range of these studies being shorter than in the bulk, and only approaching the bulk value when the distance $r \gg L$. The clear exponential character of

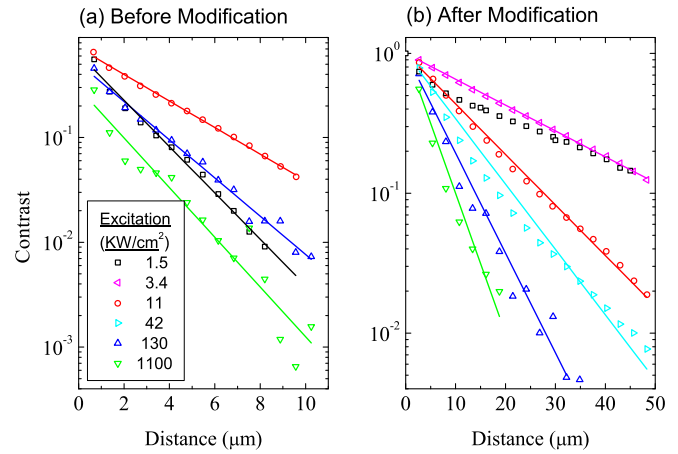


FIG. 3. Radial profiles of the PL contrast maps shown in Figs. 1 and 2.

our results, exhibited at distances up to and exceeding $5L$, confirms that the behavior is indeed exponential in our experimental configuration.

The effective diffusion lengths deduced from Fig. 3 and Fig. 4(a) are given in Fig. 4(b). While the measured lengths may differ from the one dimensional value L by a small geometrical factor (we are currently modeling this phenomenon to facilitate a more precise analysis), our measurements are generally consistent with other reports in the literature. For example, Casey, Miller, and Pinkas obtained²⁰ hole diffusion lengths of $2\text{--}4 \mu\text{m}$ and electron diffusion lengths of $7\text{--}8 \mu\text{m}$ in liquid-phase epitaxial GaAs with doping concentrations below 10^{18} cm^{-3} . Excluding the lowest excitation results where PDs become important, we find that the effective diffusion lengths are approximately 3 times larger after laser modification. If we assume that the bulk carrier lifetimes are unchanged by local deformation at the defect site, this boost in diffusion implies that the coefficient D increases by a factor of 3. We propose that the diffusion enhancement is due to a change in capture at the site. Before modification, the distribution of states and capture cross-sections at the site preferentially trap holes, while after modification electrons

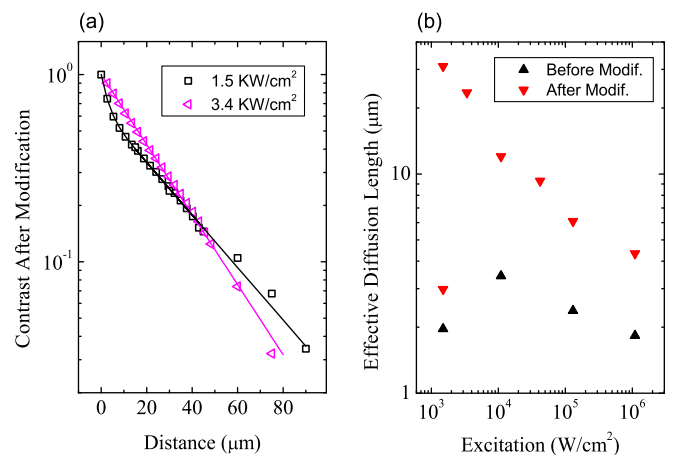


FIG. 4. (a) Detailed PL contrast profiles of the lowest excitation maps after laser modification. Note the clear change from single to double exponential behavior as the excitation intensity is reduced. (b) Effective diffusion lengths before and after modification derived from the exponential fits shown in Figs. 3 and (a). Note that the double exponential fit in (a) produces 2 effective lengths for the lowest excitation post-modification result.

become more vulnerable to trapping. For example, the defect could have a high concentration of levels below mid-gap (so as to favor holes) before, and a higher concentration of levels above midgap (so as to favor electrons) afterwards. If electrons (rather than holes) become the principal diffusion species, we would expect L to increase by a factor equal to the square root of the ratio of the mobilities: $\sqrt{20} \approx 4.5$. The difference between the observed and predicted enhancement may be attributed to ambipolar effects. Before modification, where holes lead the diffusion to the defect, the higher mobility electrons do not inhibit the hole motion appreciably. But after the high exposure event, when the defect site primarily attracts electrons, the lower mobility holes must follow. In this case, the holes inflict drag on the electron motion via the Coulomb interaction.

The divergent behavior at the lowest excitation requires a special explanation. Here, both before and after modification, we observe a sharp reduction in the effective diffusion length near the ED. Afterwards, a trickle of long-range diffusion persists, necessitating the double exponential analysis in Fig. 4(a). The long-range component maintains the trend of increased diffusion with reduced excitation and approaches the nearly 100 μm diffusion lengths measured by others²¹ in lightly doped n-type GaAs (see, Fig. 4(b)). Nevertheless, the emergence of a very short-range component is unmistakable. Since behavior in the bulk after the high exposure event should mimic bulk behavior before the event, the impeded diffusion at the lowest excitation is a more universal bulk phenomenon. Even the most pristine semiconductors contain a modicum of native point defects and elemental impurities distributed evenly throughout the crystal. When the photo-generated carrier density is low enough, localized states associated with these irregularities are available to trap electrons and/or holes, restricting their freedom to move. These traps can also operate as recombination centers, killing the radiative efficiency. Presumably, the superior electron mobility allows high-energy electrons (and not holes) to circumvent these traps and diffuse away, yielding the double exponential behavior noted above.

Since it is the even distribution of these traps (and not the diffusivity of the carrier) that limits diffusion, we cannot determine whether these bulk defects primarily trap electrons or holes. However, previous work suggests that a moderate concentration of shallow (~ 40 meV deep) electron traps and a lower concentration ($\sim 5 \times 10^{14} \text{ cm}^{-3}$) of deeper hole traps are present in the bulk of this material.⁷ At room temperature, most of the electron traps are thermally depleted, but the hole traps are deep enough to remain occupied. Hence, the PD-related hole states limit diffusion and radiative efficiency at low excitation. When these traps are filled, the model predicts a surge in the valence band population, which coincides with a steep rise in the radiative rate with increased laser power.

In conclusion, we have used confocal PL microscopy to study the diffusion of electrons and holes in the presence of

defect-related traps in GaAs over a wide range of photoexcitation conditions. A single extended defect serves as a sensor for probing the operational details. At very low excitation, diffusion and radiative efficiency are limited by trapping and nonradiative recombination at point defects distributed throughout the bulk. These states are saturated when the photoexcitation is increased, permitting long-range, lifetime-controlled diffusion to the ED. In this regime, the effective diffusion length depends on the mobility of the principal species being trapped. The exponential nature of the photoluminescence contrast profiles facilitates direct comparison of these lengths. We find that the threading dislocation in the as-grown structure primarily behaves as a hole trap, which is less detrimental because of the relatively short hole diffusion length. However, after experiencing high carrier injection, the ED is more likely to attract electrons, so its impact expands dramatically. This discovery helps explain a longstanding question on the mechanism of degradation in high-injection opto-electronics and suggests that it may be beneficial to avoid using electrons as minority carriers in the active layer of devices like high power LEDs and laser diodes.

The authors would like to thank J. J. Carapella for performing the MOVPE growth. Acknowledgment is also made to ARO/MURI, DARPA/MTO, and the Charlotte Research Institute for support of this research.

¹C. Donolato, *Optik* **52**, 19 (1978/79).

²A. Jakubowicz, *J. Appl. Phys.* **59**, 2205 (1986).

³L. Pasemann, *J. Appl. Phys.* **69**, 6387 (1991).

⁴E. B. Yakimov, *Phys. Status Solidi C* **6**, 1983 (2009).

⁵Y.-C. Fong and S. R. J. Brueck, *Appl. Phys. Lett.* **61**, 1332 (1992).

⁶W. Heinke and H. J. Queisser, *Phys. Rev. Lett.* **33**, 1082 (1974).

⁷T. H. Gfroerer, C. M. Crowley, C. M. Read, and M. W. Wanlass, *J. Appl. Phys.* **111**, 093712 (2012).

⁸R. K. Ahrenkiel, R. Ellingson, S. Johnston, and M. Wanlass, *Appl. Phys. Lett.* **72**, 3470 (1998).

⁹T. H. Gfroerer, Y. Zhang, and M. W. Wanlass, in *Proceedings of the 38th IEEE Photovoltaics Specialists Conference*, Austin, TX (IEEE, 2012), p. 1624.

¹⁰S. A. Galloway, P. R. Wilshaw, and A. Konkol, *Mater. Sci. Eng. B* **24**, 91 (1994).

¹¹P. Petroff, W. D. Johnston, and R. L. Hartman, *Appl. Phys. Lett.* **25**, 226 (1974).

¹²P. Petroff and R. L. Hartman, *Appl. Phys. Lett.* **23**, 469 (1973).

¹³B. Monemar, R. M. Potemski, M. B. Small, J. A. Van Vechten, and G. R. Woolhouse, *Phys. Rev. Lett.* **41**, 260 (1978).

¹⁴G. Cox, D. Szyzka, U. Poppe, K. H. Graf, K. Urban, C. Kisielowski-Kemmerich, J. Kruger, and H. Alexander, *Phys. Rev. Lett.* **64**, 2402 (1990).

¹⁵Ph. Ebert, C. Domke, and K. Urban, *Appl. Phys. Lett.* **78**, 480 (2001).

¹⁶*IMAGEJ* is a public domain, Java-based image processing program developed at the National Institutes of Health.

¹⁷D. Cherns, S. J. Henley, and F. A. Ponce, *Appl. Phys. Lett.* **78**, 2691 (2001).

¹⁸N. Pauc, M. R. Phillips, V. Aimez, and D. Drouin, *Appl. Phys. Lett.* **89**, 161905 (2006).

¹⁹E. B. Yakimov, *Appl. Phys. Lett.* **97**, 166101 (2010).

²⁰H. C. Casey, Jr., B. I. Miller, and E. Pinkas, *J. Appl. Phys.* **44**, 1281 (1973).

²¹A. Nemcsics and K. Somogyi, in *Proceedings of the Third International EuroConference on Advanced Semiconductor Devices and Microsystems*, Smolenice Castle, Slovakia (IEEE, 2000), p. 265.